Alternate routes to the cell surface underpin insulin-regulated membrane trafficking of GLUT4

Dimitrios Kioumourtzoglou[1,2], Paul R. Pryor[2,3], Gwyn W. Gould[1] and Nia J. Bryant[1,2]

[1] Institute of Molecular, Cell and Systems Biology, College of Medical, Veterinary and Life Sciences, University of Glasgow, G12 8QQ, United Kingdom.

[2] Department of Biology, University of York, YO10 5DD, United Kingdom.

[3]Centre for Immunology and Infection, Hull York Medical School, University of York, YO10 5DD, United Kingdom.

Correspondence should be addressed to:

nia.bryant@york.ac.uk, Tel; +44(0) +44(0)1904-328622, Fax: +44(0)1904-328505

and/or

gwyn.gould@glasgow.ac.uk, Tel; +44(0)141-330-5263, Fax: +44(0)141-330-5481

JCS Advance Online Article. Posted on 12 June 2015

Abstract

Insulin-stimulated delivery of glucose transporters (GLUT4) from specialized intracellular GLUT4 storage vesicles (GSVs) to the surface of fat and muscle cells is central to whole-body glucose. This translocation and subsequent internalization of GLUT4 back into intracellular stores transits numerous small membrane-bound compartments (internal GLUT4-containing vesicles; IGVs) including GSVs, but the function of these different compartments is not clear. Cellugyrin and sortilin define distinct populations of IGV; sortilin-positive IGVs represent GSVs, but the function of cellugyrin-containing IGVs is unknown. Here we demonstrate a role for cellugyrin in intracellular sequestration of GLUT4 in HeLa cells and have used a proximity ligation assay to follow changes in pairwise associations between cellugyrin, sortilin, GLUT4 and membrane trafficking machinery following insulin-stimulation of 3T3-L1 adipoctyes. Our data suggest that insulin stimulates traffic from cellugyrin- to sortilin- membranes, and that cellugyrin-IGVs provide an insulin-sensitive reservoir to replenish GSVs following insulin-stimulated exocytosis of GLUT4. Furthermore, our data support the existence of a pathway from cellugyrin-membranes to the surface of 3T3-L1 adipocytes that bypasses GSVs under basal conditions, and that insulin diverts traffic away from this into GSVs.

Introduction

Insulin reduces elevated plasma glucose levels by increasing glucose transport into fat and muscle through the facilitative glucose transporter GLUT4. In the absence of insulin ~95% of GLUT4 localises to intracellular compartments with insulin causing redistribution to the plasma membrane (PM) (Bryant and Gould, 2011; Bryant et al., 2002). This is disrupted in insulin-resistance underlying Type-2 diabetes.

GLUT4 cycles through the surface of insulin-sensitive cells in both the presence and absence of insulin (Bryant et al., 2002; Kandror and Pilch, 2011). In the absence of insulin, GLUT4 is efficiently internalized into early/recycling endosomes from where it traffics to insulin-responsive, GLUT4-storage, vesicles (GSVs) (Kandror and Pilch, 2011). Insulin increases the amount of GLUT4 at the PM by dramatically increasing exocytosis from GSVs mediated, in part, by formation of a complex between the GSV-resident v-SNARE VAMP2 and its cognate t-SNARE on the PM (Bryant and Gould, 2011; Bryant et al., 2002).

The intimate association of GSVs with the dynamic endosomal system makes their characterization challenging (Bryant et al., 2002; Kandror and Pilch, 2011). Morphological/biochemical studies indicate that, under basal conditions, the majority of GLUT4 resides in small tubulo-vesicular structures (Bryant et al., 2002; Kandror and Pilch, 2011). It is from a subpopulation of these internal GLUT4-containing vesicular structures (IGVs) that GLUT4 mobilises to the PM in response to insulin; these by definition represent insulin-responsive GSVs (Bryant et al., 2002; Kandror and Pilch, 2011). Two populations of IGVs can be separated by density gradient fractionation (Jedrychowski et al., 2010; Kupriyanova and Kandror, 2000; Kupriyanova et al., 2002). Both contain GLUT4 and other proteins that translocate to the PM of adipocytes in an insulin-dependent manner, including VAMP2 and the insulin-responsive aminopeptidase, but can be distinguished by the presence/absence of the multi-ligand sorting receptor sortilin and the protein cellugyrin (Jedrychowski et al., 2010; Kupriyanova and Kandror, 2000; Kupriyanova et al., 2002). Sortilin plays a key role in GSV biogenesis (Huang et al., 2013; Shi and Kandror, 2005) and like other GSV-residents translocates to the PM in response to insulin; supporting the notion that sortilin-positive (cellugyrin-negative) IGVs represent GSVs (Jedrychowski et al., 2010; Kupriyanova and Kandror, 2000; Kupriyanova et al.,

2002). In contrast, cellugyrin does not translocate to the PM in response to insulin and the function of cellugyrin-positive (sotillin-negative) IGVs is unknown (Jedrychowski et al., 2010; Kim and Kandror, 2012; Kupriyanova and Kandror, 2000; Kupriyanova et al., 2002; Li et al., 2009).

The data presented here are consistent with a model whereby, in addition to its well-studied role of stimulating traffic from GSVs to the cell surface, insulin regulates traffic between distinct populations of internal GLUT4-containing membranes (Xu and Kandror, 2002). We propose basal traffic from cellugyrin-positive vesicles to the PM is rerouted to sortilin-positive GSVs upon insulin-stimulation. We also demonstrate a role for cellugyrin in intracellular sequestration of GLUT4 and suggest that this provides a reservoir to replenish GSVs following insulin-stimulation.

Results and Discussion

Insulin-regulates traffic between cellugyrin and sortilin-containing compartments

To investigate the relationship between sortilin-positive and cellugyrin-positive IGVs we used an *in situ* proximity ligation assay (PLA). PLA uses antibody detection to determine whether proteins are in close proximity (Fredriksson et al., 2002; Soderberg et al., 2006). Secondary antibodies, with specific single-stranded oligonucleotides attached, detect primary antibodies bound to the proteins of interest (Fredriksson et al., 2002). If the proteins are in close proximity, the binding of the secondary antibodies allows hybridisation of connector oligonucleotides; enzymatic ligation then forms a circular ssDNA molecule providing a template for rolling circle amplification primed by one of the oligonucleotides from the secondary antibodies (Soderberg et al., 2006). The product of this can be detected using fluorescent oligonucleotide probes, allowing the frequency of each protein-protein association to be measured using microscopy (Soderberg et al., 2006).

We have previously used PLA to study insulin-dependent formation of Syntaxin4-containing SNARE complexes (Kioumourtzoglou et al., 2014). However, proteins need not be part of the same complex to give a signal, the assay simply requires that they are within close proximity, the distance reflecting the size of the antibodies and oligonucleotides used. The maximum distance between epitopes able to give a PLA signal (represented as a fluorescent dot ~500nm) is estimated at 30 nm (Soderberg et al., 2006), including the size of the two antibodies (F_{ab}=7 nm) and the coupled oligonucleotides (~40 nucleotides) (Fredriksson et al., 2002). Given the diameter of GSVs (~ 50nm, see Bryant et al., 2002), any two proteins located on the surface of the same quadra-sphere are potentially detectable by PLA. It is important to note that the fluorescent signal does not report on the localization of the associated proteins due to the nature of the assay, but rather reports on the extent of their associations (Fredriksson et al., 2002).

Consistent with fractionation studies demonstrating that sortilin and cellugyrin populate distinct populations of IGVs (Jedrychowski et al., 2010; Kupriyanova and Kandror, 2000) and the localization of VAMP2 to IGVs (Martin et al., 1997; Martin et al., 1996), both cellugyrin and sortilin give PLA signal with the v-SNARE VAMP2

but not with each other (Figure 1). This does not provide definitive evidence that the two proteins reside in distinct IGV populations, but is noteworthy as the detection antibodies used both give PLA signal with VAMP2 (Figure 1) which is found in both cellugyrin- and sortilin-positive vesicles (Jedrychowski et al., 2010; Kupriyanova and Kandror, 2000).

The number of PLA puncta is proportional to the number of associations between two proteins (Soderberg et al., 2006), but it is not possible to compare numbers of associations between different protein pairs due to variability in antibody affinity/avidity. Comparisons can, however, be made between changes in associations of the same pairs of proteins using the same antibodies (Kioumourtzoglou et al., 2014). Five minutes after insulin treatment of adipocytes, a significant decrease was observed in associations of cellugyrin with both GLUT4 and VAMP2, with concomitant increases between sortilin and GLUT4/VAMP2 (Figure 1), consistent with the notion that acute insulin treatment stimulates GLUT4 traffic from cellugyrin- to sortilin-positive vesicles.

While sortilin-positive GSVs are the source of GLUT4 delivered to the PM following short-term exposure to insulin (~5 minutes), GLUT4 exocytosis after longer times (~20 minutes) appears to involve recycling from endosomes (Xu et al., 2011); Chen et al., 2012). To investigate these temporal differences, we extended our PLA analyses to include 20 minutes after insulin challenge (Figure 1). In contrast to the reduction in associations between cellugyrin and GLUT4/VAMP2 following short-term (5 minutes) exposure to insulin, GLUT4/cellugyrin associations increase (Figure 1), consistent with this set of IGVs being replenished as GLUT4 recycles from the PM (Xu et al., 2011; Chen et al., 2012). This model is also supported by the observation that cellugyrin-positive vesicles accumulate recycling proteins, e.g. transferrin receptor, internalized from the cell surface (Kupryanova et al, 2002).

Distinct pools of internal membranes provide the source of GLUT4 traffic to the cell surface under basal and insulin-stimulated conditions

The observation that insulin stimulates translocation of sortilin, but not cellugyrin, to the PM provided the first evidence that the two biochemically-identified populations of IGVs are functionally distinct (Shi and Kandror, 2005). The data in Figure 1 build

on this and suggest that cellugyrin-positive vesicles provide a reservoir for replenishment of (sortilin-positive) GSVs upon insulin-stimulation, a model consistent with studies demonstrating that while cellugyrin doesn't translocate to the cell surface, GLUT4 is lost from the cellugyrin-positive compartment in response to insulin (Jedrychowski et al., 2010; Shi and Kandror, 2005).

To understand better how insulin-regulates traffic to the cell surface, we asked whether cargo from cellugyrin-positive internal membranes transits through sortilin-positive (cellugyrin-negative) vesicles en route to the PM under basal as well as insulin-stimulated conditions. If this were the case cellugyrin would not encounter PM t-SNAREs. Figure 2 shows that this is not so as cellugyrin gives PLA signal with SNAP23 (and Syntaxin4; Fig. S2). It is important to note that although relatively few associations of cellugyrin with SNAP23/Syntaxin4 were detected per cell these represent real signal that disappears after 5 minutes insulin-stimulation (Figs 2 and S2). Consistent with reports that sortilin translocates to the PM along with other GSV residents in response to insulin but cellugyrin does not (Kim and Kandror, 2012; Kupriyanova and Kandror, 2000), an increase in associations between sortilin and SNAP23 and Syntaxin4 (Figs. 2 and S2) was observed concomitant with the reduction of cellugyrin/cell surface tSNARE associations at 5 minutes after insulin treatment (Figs 2 and S2). This supports the existence of direct traffic from cellugyrin-positive (sortilin-negative) membranes to the PM under basal conditions and, taken in conjunction with data in Figure 1, indicates that acute insulin challenge diverts traffic from this pathway to that mediated via sortilin-positive (cellugyrin-negative) vesicles. At longer times after insulin treatment, the cellugyrin/SNAP23 associations revert to basal levels (Figure 2), consistent with this cellugyrin-positive set of IRVs being involved in the recycling of GLUT4 back to the PM. We speculate that this corresponds to endosomal recycling of GLUT4 as described by Xu et al, 2011 and Chen et al., 2013, consistent with the observation that transferrin receptors recycle through cellugyrin-positive vesicles (Kupriyanova et al., 2002). Concomitant alterations in sortilin/tSNARE associations are also consistent with this (Figure 2).

Basal adipocytes contain two distinct pools of Syntaxin4, one in complex with SNAP23, the other with VAMP2 and Munc18c (Kioumourtzoglou et al., 2014). Direct interaction between VAMP2 and Syntaxin4 in the absence of SNAP23 is

inhibitory to SNARE complex formation, an effect alleviated *in vitro* by a phosphomimetic (Y521E) version of the regulatory protein Munc18c but not the wild-type (Kioumourtzoglou et al., 2014). These data led to the model that the two pools of Syntaxin4 are functionally distinct; that in complex with SNAP23 facilitating basal recycling, the other providing a pool of Syntaxin4 held inactive through interaction with VAMP2 that can be rapidly mobilised by insulin through Munc18c phosphorylation (Kioumourtzoglou et al., 2014). The simplest model integrating the data in Figures 1 and 2 into this is that recycling through the PM under basal conditions involves cellugyrin-positive (but not sortilin-positive) vesicles whereas insulin-stimulated delivery to the PM, achieved by release of Syntaxin4 from the Syntaxin4/VAMP2/Munc18c pool, involves sortilin-positive vesicles. Consistent with this Munc18c is associated with sortilin vesicles, but not those marked by cellugyrin (Figure 3).

Cellugyrin plays a role in intracellular sequestration of GLUT4

Cellugyrin (synaptogyrin-2), one of 4 gyrin family members related to the physin and SCAMP families (Hubner et al., 2002; Kupriyanova and Kandror, 2000), is ubiquitously expressed (Hubner et al., 2002; Kupriyanova and Kandror, 2000). Little is known about cellugyrin (or any gyrin) function, but a role in vesicle biogenesis has been implicated since overexpression increases numbers of synaptic-like microvesicles in PC12 cells (Belfort et al., 2005), and flies lacking synaptogyrin have increased synaptic vesicle diameter (Stevens et al., 2012).

We identified a short sequence within the N-terminal tail of cellugyrin similar to that required for trafficking of other endosomal proteins (Seaman, 2007). Mutation of this (FDL/AAA) changes localization of tdTomato-tagged cellugyrin from cytosolic puncta, characteristic of endosomal proteins, to the surface of HeLa cells (Fig. 4).

When HA-GLUT4-GFP (Muretta et al., 2008) is expressed in a variety of cell types, including HeLas, that do not normally express GLUT4, an intracellular localization with exclusion from the plasma membrane similar to that in fat and muscle cells under basal conditions is observed (Haga et al., 2011). The HA-epitope is in an extracellular loop and thus only HA-GLUT4-GFP inserted into the PM is accessible to HA-antibody in absence of cell permeabilisation. HeLa cells expressing PM localized

cellugyrin$_{FDL/AAA}$ display increased levels of surface HA-GLUT4-GFP (Fig. 4), demonstrating that cellugyrin localization is important for determining the localization of GLUT4. Given that cellugyrin localizes to intracellular vesicles, we propose that cellugyrin plays a role in the intracellular sequestration of GLUT4. Overexpression of either wild type or mutant (FDL/AAA) cellugyrin did not affect the levels of HA-GLUT4-GFP in HeLa cells (Fig. S3).

Concluding remarks

The data presented here are consistent with a model in which, in addition to increasing delivery of GLUT4 to the PM insulin also stimulates traffic between distinct populations of internal GLUT4 containing vesicles (IGVs): from cellugyrin-positive to sortilin-positive vesicles. Consistent with this are reports that unlike sortilin cellugyrin doesn't translocate to the PM in response to insulin, and insulin triggers a reduction in the amount of GLUT4 in cellugyrin-positive membranes (Jedrychowski et al., 2010; Shi and Kandror, 2005). These data support a model whereby sortilin-positive membranes are the source of GLUT4 delivered to the PM in response to insulin and that cellugyrin-positive vesicles serve as a reservoir to replenish this pool. Although PLA does not report on the dynamics of trafficking events, our demonstration of associations between cellugyrin and the cell surface t-SNAREs under basal, but not acute insulin-stimulated conditions extend this, and indicate that cellugyrin-positive membranes are the source of traffic through the PM under basal conditions (Figure 2). Consistent with our contention that insulin diverts traffic from here to sortilin-positive GSVs is the dramatic increase in associations of sortilin with Syntaxin4/SNAP23 in response to acute insulin challenge (Figure 2).

Figures 1 and 2 support the existence of two functionally distinct GLUT4 trafficking pathways to the PM: from cellugyrin-positve membranes to the cell surface under basal conditions; and from cellugyrin- to sortilin-positive membranes and then to the PM following acute insulin-stimulation. The notion of distinct GLUT4 trafficking pathways under basal and insulin conditions is supported by studies in adipocytes from transgenic mice overexpressing GLUT4, where the amount of GLUT4 at the plasma membrane under basal conditions is elevated four-fold compared to those from wild-type but only by a factor of two following insulin-stimulation (Carvalho et al., 2004). Our PLA data also reveal important differences in GLUT4 trafficking at

longer times after insulin challenge. After delivery of GSVs to the PM following acute insulin treatment, GLUT4 recycles between the PM and IRVs; these different trafficking routes were identified using VAMP2-pHlorin as a reporter (Xu et al., 2011), and have been shown to involve distinct Rab proteins (Chen et al 2013). Our data further highlight mechanistic differences between these routes to the PM, as GLUT4 recycling at longer times of insulin challenge involves cellugyrin-positive vesicles.

We recently reported the presence of two distinct pools of Syntaxin4 in adipocytes under basal conditions, one in complex with SNAP23, the other with VAMP2 and Munc18c (Kioumourtzoglou et al., 2014). We suggested that the latter is mobilised, through Munc18c in response to insulin. Figure 3 shows that Munc18c does indeed participate in insulin-stimulated delivery of sortilin-membranes to the PM. Unlike its associations with the PM t-SNAREs (Figs. 2 and S1) and VAMP2 (Fig 1), associations of sortilin with Munc18c do not increase in number in response to insulin (Fig 3), suggesting that levels of Munc18c may be limiting for insulin-regulated traffic to the PM. This is consistent with the reported role of Munc18c phosphorylation as a regulatory switch in this process (Aran et al., 2011; Jewell et al., 2011; Kioumourtzoglou et al., 2014).

Our model predicts a fraction of GSVs are pre-docked at the PM through Syntaxin4-VAMP2 interactions (Kioumourtzoglou et al., 2014). This would allow rapid insertion of GLUT4 into the PM in response to insulin, via phosphorylation of Munc18c (Kioumourtzoglou et al., 2014). This is consistent with TIRF microscopy studies demonstrating a large proportion of GLUT4 is within 100nm of the PM under basal conditions in primary adipocytes (Stenkula et al., 2010), and the marked diminution of GLUT4-positive vesicles located at the periphery of 3T3-L1 adipocytes in response to insulin (Bai et al., 2007; Hatakeyama and Kanzaki, 2011), although it is important to note that the sortilin/cellugyrin status of these GLUT4-positive vesicles has not been established. After insulin-stimulation these GSVs must be replenished. We propose that cellugyrin-positive membranes provide a reservoir of GLUT4 for this. In support of this we provide evidence for a role of cellugyrin in intracellular sequestration of GLUT4 and suggest that insulin stimulates traffic between cellugyrin-positive and sortilin-positive membranes.

Materials and Methods

Proximity ligation assay (PLA)

PLA was performed as described using the Duolink® system (Sigma-Aldrich) as described (Kioumourtzoglou et al., 2014) (see Figure S1 for further details of assay conditions and data analysis and Table S1 for antibodies used).

Expression constructs

tdTomato-Cellugyrin was made by excising GFP from pEGFP-C3 (NheI/EcoRI) and inserting tdTomato and rCellugyrin PCR products using In-Fusion cloning (Clontech). tdTomato-Cellugyrin$_{FDL>AAA}$ was made using site-directed mutagenesis.

Acknowledgments

We thank Cynthia Corely Mastick (University of Nevada) for the HA-GLUT4-GFP vector, Roger Tsien (UCSD) for tdTomato and Konstantin Kandror (Boston University) for rat cellugyrin. This work was supported by Diabetes-UK (11/0004289) and a BBSRC Doctoral Training Programme (BB/F016735/1). NJB is a Lister Institute of Preventive Medicine Prize Fellow.

References

Aran, V., N.J. Bryant, and G.W. Gould. (2011). Tyrosine phosphorylation of Munc18c on residue 521 abrogates binding to Syntaxin 4. *BMC Biochem*. **12,** 19.

Bai, L., Y. Wang, J. Fan, Y. Chen, W. Ji, A. Qu, P. Xu, D.E. James, and T. Xu. (2007). Dissecting multiple steps of GLUT4 trafficking and identifying the sites of insulin action. *Cell Metab*. **5,** 47-57.

Belfort, G.M., K. Bakirtzi, and K.V. Kandror. (2005). Cellugyrin induces biogenesis of synaptic-like microvesicles in PC12 cells. *J. Biol. Chem*. **280,** 7262-7272.

Bryant, N.J., and G.W. Gould. (2011). SNARE Proteins Underpin Insulin-Regulated GLUT4 Traffic. *Traffic*. **12,** 657-664.

Bryant, N.J., R. Govers, and D.E. James. (2002). Regulated transport of the glucose transporter GLUT4. *Nat. Rev. Mol. Cell Biol*. **3,** 267-277.

Carvalho, E., S.E. Schellhorn, J.M. Zabolotny, S. Martin, E. Tozzo, O.D. Peroni, K.L. Houseknecht, A. Mundt, D.E. James, and B.B. Kahn. (2004). GLUT4 overexpression or deficiency in adipocytes of transgenic mice alters the composition of GLUT4 vesicles and the subcellular localization of GLUT4 and insulin-responsive aminopeptidase. *J. Biol. Chem*. **279,** 21598-21605.

Chen, Y., Y. Wang, J. Zhang, Y. Deng, L. Jiang, E. Song, X.S. Wu, J.A. Hammer, T. Xu, and J. Lippincott-Schwartz. (2012). Rab10 and myosin-Va mediate insulin-stimulated GLUT4 storage vesicle translocation in adipocytes. *J. Cell Biol*. **198,** 545-560.

Fredriksson, S., M. Gullberg, J. Jarvius, C. Olsson, K. Pietras, S.M. Gustafsdottir, A. Ostman, and U. Landegren. (2002). Protein detection using proximity-dependent DNA ligation assays. *Nat Biotechnol*. **20,** 473-477.

Haga, Y., K. Ishii, and T. Suzuki. (2011). N-glycosylation is critical for the stability and intracellular trafficking of glucose transporter GLUT4. *J. Biol. Chem*. **286,** 31320-31327.

Hatakeyama, H., and M. Kanzaki. (2011). Molecular basis of insulin-responsive GLUT4 trafficking systems revealed by single molecule imaging. *Traffic*. **12,** 1805-1820.

Huang, G., D. Buckler-Pena, T. Nauta, M. Singh, A. Asmar, J. Shi, J.Y. Kim, and K.V. Kandror. (2013). Insulin responsiveness of glucose transporter 4 in 3T3-L1 cells depends on the presence of sortilin. *Mol. Biol. Cell*. **24,** 3115-3122.

Hubner, K., R. Windoffer, H. Hutter, and R.E. Leube. (2002). Tetraspan vesicle membrane proteins: synthesis, subcellular localization, and functional properties. *Int. Rev. Cytol*. **214,** 103-159.

Jedrychowski, M.P., C.A. Gartner, S.P. Gygi, L. Zhou, J. Herz, K.V. Kandror, and P.F. Pilch. (2010). Proteomic analysis of GLUT4 storage vesicles reveals LRP1 to be an important vesicle component and target of insulin signaling. *J. Biol. Chem*. **285,** 104-114.

Jewell, J.L., E. Oh, L. Ramalingam, M.A. Kalwat, V.S. Tagliabracci, L. Tackett, J.S. Elmendorf, and D.C. Thurmond. (2011). Munc18c phosphorylation by the insulin receptor links cell signaling directly to SNARE exocytosis. *J. Cell Biol*. **193,** 185-199.

Kandror, K.V., and P.F. Pilch. (2011). The sugar is sIRVed: sorting Glut4 and its fellow travelers. *Traffic*. **12,** 665-671.

Kim, J.Y., and K.V. Kandror. (2012). The first luminal loop confers insulin responsiveness to glucose transporter 4. *Mol. Biol. Cell*. **23,** 910-917.

Kioumourtzoglou, D., G.W. Gould, and N.J. Bryant. (2014). Insulin stimulates syntaxin4 SNARE complex assembly via a novel regulatory mechanism. *Mol. Cell. Biol*. **34,** 1271-1279.

Kupriyanova, T.A., and K.V. Kandror. (2000). Cellugyrin is a marker for a distinct population of intracellular Glut4-containing vesicles. *J. Biol. Chem*. **275,** 36263-36268.

Kupriyanova, T.A., V. Kandror, and K.V. Kandror. (2002). Isolation and characterization of the two major intracellular Glut4 storage compartments. *J. Biol. Chem*. **277,** 9133-9138.

Li, L.V., K. Bakirtzi, R.T. Watson, J.E. Pessin, and K.V. Kandror. (2009). The C-terminus of GLUT4 targets the transporter to the perinuclear compartment but not to the insulin-responsive vesicles. *Biochem. J*. **419,** 105-112, 101 p following 112.

Martin, S., J.E. Rice, G.W. Gould, S.R. Keller, J.W. Slot, and D.E. James. (1997). The glucose transporter GLUT4 and the aminopeptidase vp165 colocalise in tubulo-vesicular elements in adipocytes and cardiomyocytes. *J Cell Sci*. **110,** 2281-2291.

Martin, S., J. Tellam, C. Livingstone, J.W. Slot, G.W. Gould, and D.E. James. (1996). The glucose transporter (GLUT-4) and vesicle-associated membrane protein-2 (VAMP-2) are segregated from recycling endosomes in insulin-sensitive cells. *J Cell Biol*. **134,** 625-635.

Muretta, J.M., I. Romenskaia, and C.C. Mastick. (2008). Insulin releases Glut4 from static storage compartments into cycling endosomes and increases the rate constant for Glut4 exocytosis. *J. Biol. Chem*. **283,** 311-323.

Oh, E., B.A. Spurlin, J.E. Pessin, and D.C. Thurmond. (2005). Munc18c heterozygous knockout mice display increased susceptibility for severe glucose intolerance. *Diabetes*. **54,** 638-647.

Seaman, M.N. (2007). Identification of a novel conserved sorting motif required for retromer-mediated endosome-to-TGN retrieval. *J. Cell Sci*. **120,** 2378-2389.

Shi, J., and K.V. Kandror. (2005). Sortilin is essential and sufficient for the formation of Glut4 storage vesicles in 3T3-L1 adipocytes. *Dev Cell*. **9,** 99-108.

Soderberg, O., M. Gullberg, M. Jarvius, K. Ridderstrale, K.J. Leuchowius, J. Jarvius, K. Wester, P. Hydbring, F. Bahram, L.G. Larsson, and U. Landegren. (2006). Direct observation of individual endogenous protein complexes in situ by proximity ligation. *Nat Methods*. **3,** 995-1000.

Stenkula, K.G., V.A. Lizunov, S.W. Cushman, and J. Zimmerberg. (2010). Insulin controls the spatial distribution of GLUT4 on the cell surface through regulation of its postfusion dispersal. *Cell Metab*. **12,** 250-259.

Stevens, R.J., Y. Akbergenova, R.A. Jorquera, and J.T. Littleton. (2012). Abnormal synaptic vesicle biogenesis in Drosophila synaptogyrin mutants. *J. Neurosci.* **32,** 18054-18067, 18067a.

Thurmond, D.C., B.P. Ceresa, S. Okada, J.S. Elmendorf, K. Coker, and J.E. Pessin. (1998). Regulation of insulin-stimulated GLUT4 translocation by Munc18c in 3T3L1 adipocytes. *J. Biol. Chem*. **273,** 33876-33883.

Xu, Y., B.R. Rubin, C.M. Orme, A. Karpikov, C. Yu, J.S. Bogan, and D.K. Toomre. (2011). Dual-mode of insulin action controls GLUT4 vesicle exocytosis. *J. Cell Biol*. **193,** 643-653.

Xu, Z., and K.V. Kandror. (2002). Translocation of small preformed vesicles is responsible for the insulin activation of glucose transport in adipose cells. Evidence from the in vitro reconstitution assay. *J. Biol. Chem*. **277,** 47972-47975.

Figures

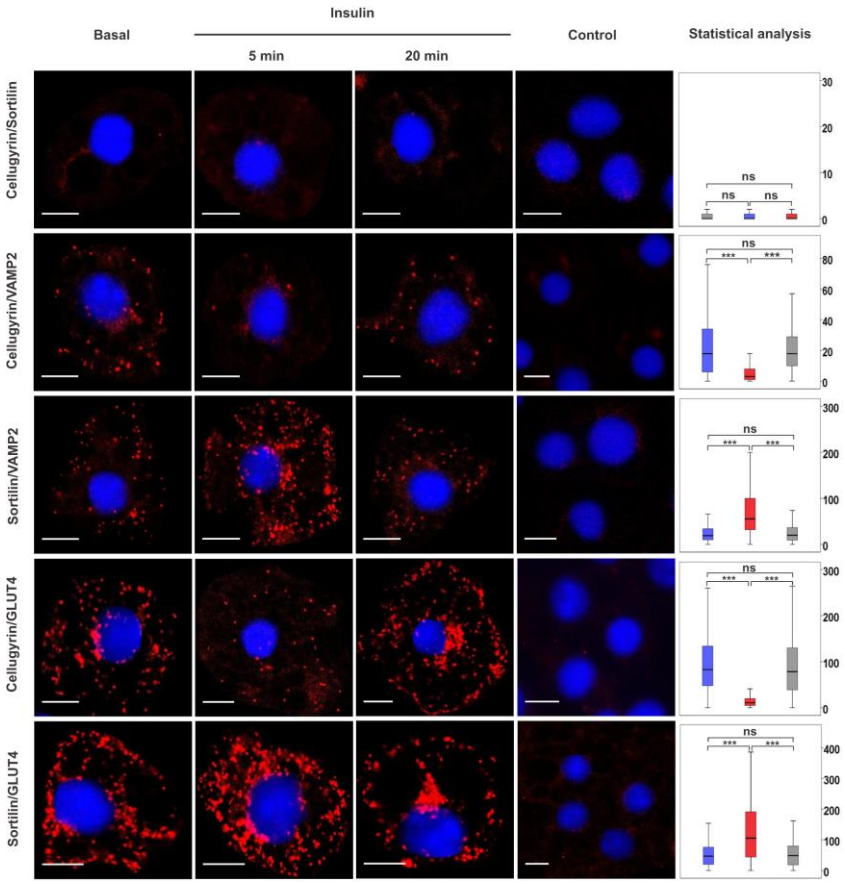

Figure 1. *Pairwise associations between Cellugyrin, Sortilin and VAMP2 or GLUT4 in the presence and absence of insulin-stimulation*. PLA was used to detect pairwise associations between Cellugyrin, Sortilin and VAMP2 or GLUT4 in 3T3-L1 adipocytes treated with 100nM insulin for 5 or 20 min as indicated (Insulin) or not (Basal). PLA signals shown in red, DAPI stain in blue. Controls omitting the first listed primary antibody are shown (controls omitting either and both primary antibodies were performed in parallel with no significant signal detected). Statistical analyses of PLA data were performed using Blobfinder and SPSS software. Boxplots represent median number of signals and quartile range of 200-300 cells per condition (y-axis; blue = basal, red = 5 min, grey=20 min insulin stimulation). Images are representative of 3 independent experiments. For all control experiments, the median PLA signal value was <1 per cell. Any median signal >1 obtained in the presence of both primary antibodies was found to be significantly greater than that obtained in controls for all combinations shown ns= $p \geq 0.05$, *** = $p < 0.001$. Scale bars = 10μm

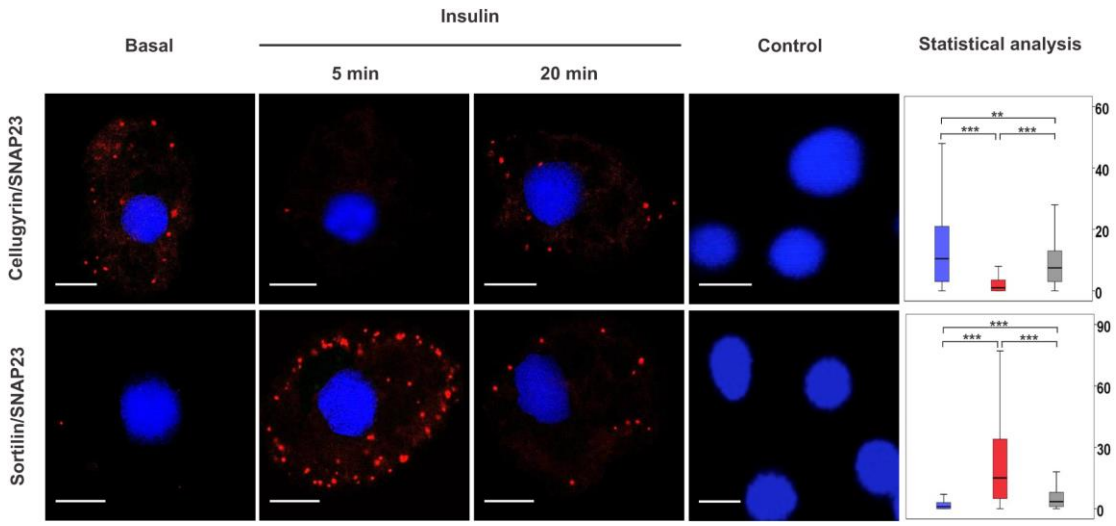

Figure 2. *Associations of SNAP23 with Cellugyrin and Sortilin in the presence and absence of insulin-stimulation*. PLA was used to detect pairwise associations of SNAP23 with either Cellugyrin or Sortilin in 3T3-L1 adipocytes treated with 100nM insulin for 5 or 20 min, as indicated (Insulin) or not (Basal). PLA signals shown in red, DAPI stain in blue. Images are representative of 3 independent experiments. Data were analysed as for Figure 1 (y-axis; blue = basal, red = 5 min and grey = 20 min insulin stimulation respectively. ns= $p \geq 0.05$, *** = $p < 0.001$, ** = $0.001 \leq p < 0.05$). Scale bars = 10µm.

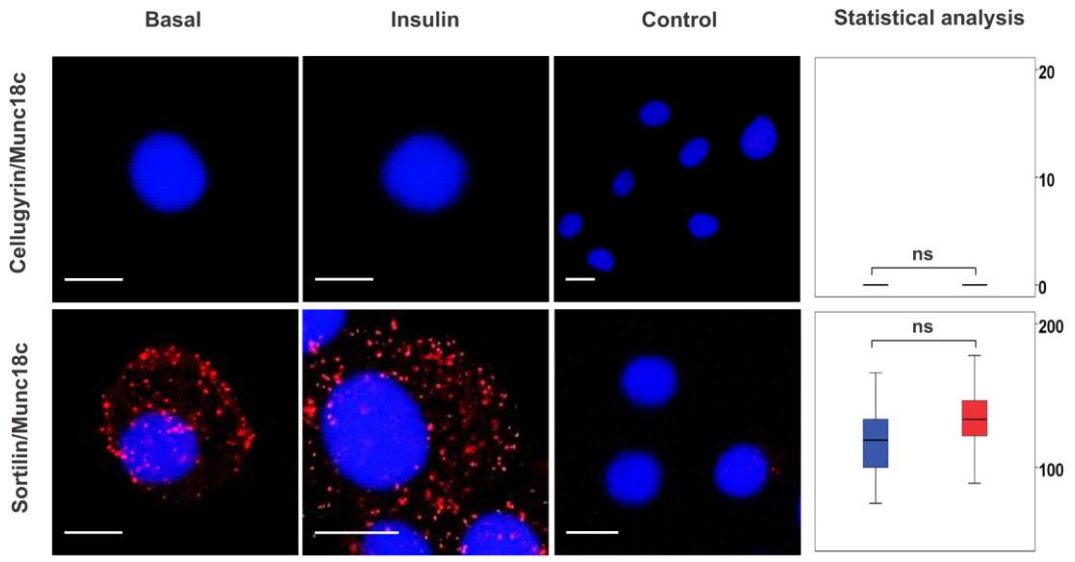

Figure 3. *Pairwise associations between Cellugyrin, Sortilin and Munc18c in the presence and absence of insulin-stimulation*. PLA was used to detect pairwise associations between Cellugyrin, Sortilin and Munc18c in 3T3-L1 adipocytes treated with 100nM insulin for 5 min (Insulin) or not (Basal). PLA signals shown in red, DAPI stain in blue. Data were analysed and represented as for Figure 1; (y-axis; blue = basal, red = 5 min insulin stimulation respectively. ns = $p \geq 0.05$). Scale bars = 10μm.

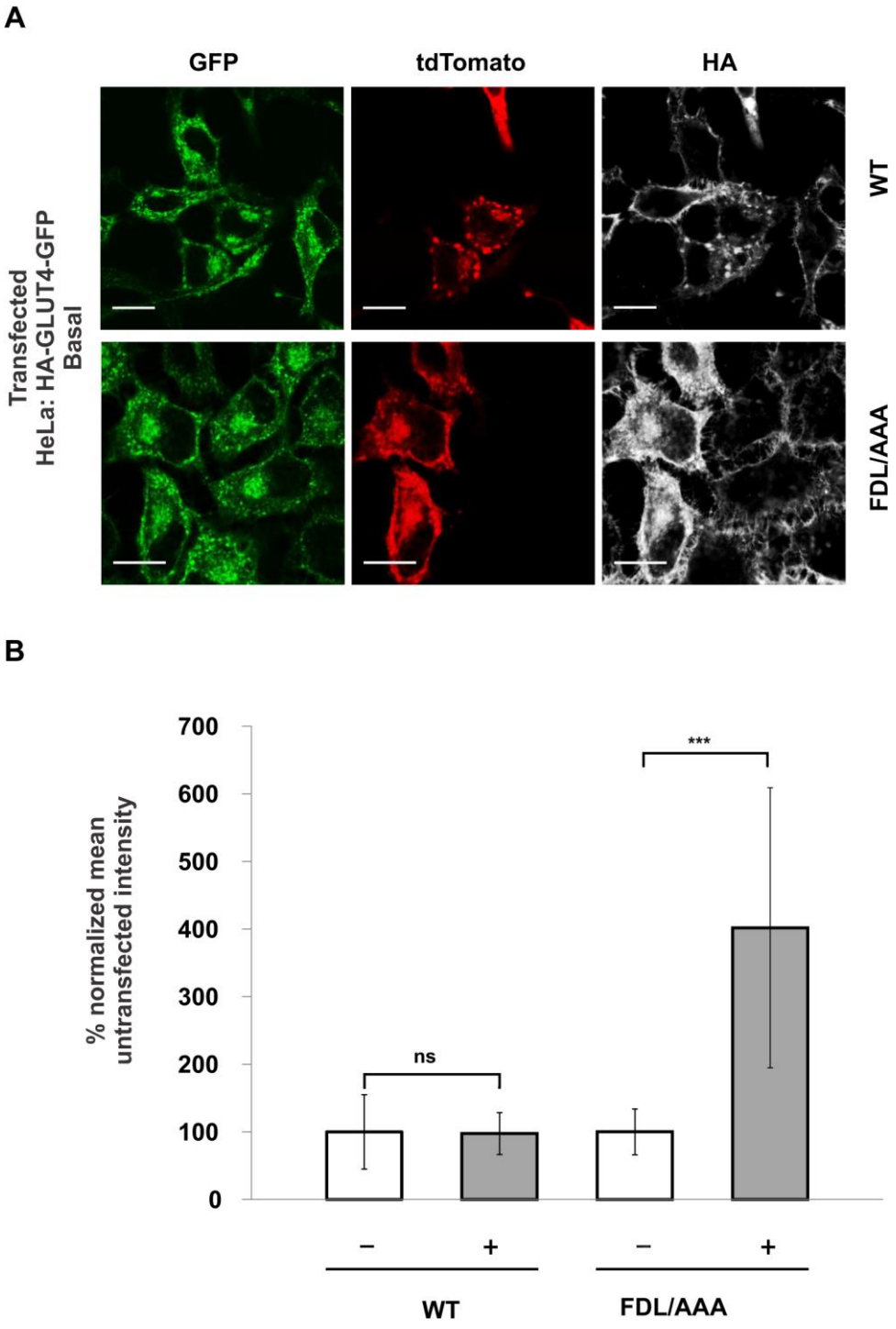

Figure 4. (A) *Mutation of a short sorting sequence within the N-terminal cytosolic tail of cellugyrin (FDL/AAA) results in mislocalisation to the plasma membrane and loss of intracellular sequestration of GLUT4*. A HeLa cell line stably expressing HA-GLUT4-GFP was created following infection with a lentiviral construct encoding GFP-tagged GLUT4 carrying an HA epitope in the first extracellular loop (Muretta et al., 2008). These were subsequently transiently transfected with an expression vector

encoding either wild-type (WT) or mutant (FDL/AAA) tdTomato-tagged cellugyrin. Indirect immunofluorescence was used to detect HA-GLUT4-GFP at the plasma membrane by staining in the absence of cell permeabilisation (pseudo-coloured, white). Expression and localization of the tdTomato-tagged cellugyrin construct is shown in red and the total amount of HA-GLUT4-GFP in green. Images are representative of three independent experiments. Scale bars = 10μm **(B)** Quantification of indirect HA-GLUT4-GFP immunofluorescence (pseudo-coloured, white) at the plasma membrane was normalized to total GLUT4-GFP fluorescence from cells transfected with either WT or FDL/AAA tdTomato-tagged cellugyrin-encoding vectors (see panel A). The ratio of surface/total GLUT4 staining is compared between transfected (+) and non-transfected (-) cells from the same coverslip, and shows that surface levels of HA-GLUT4-GFP are increased in cells expressing FDL>AAA cellugyrin. Error bars represent standard deviations from 10 different cells (data statistically analyzed in pairs using a two-tailed *t* test; ns= $p \geq 0.05$, *** = $p < 0.001$.). Quantification of GFP signal from cells expressing either WT or FDL>AAA cellugyrin revealed no difference in total GLUT4-GFP levels between the two (Fig. S3).

Figure S1. *Schematic representation of Proximity Ligation Assay to examine pairwise associations between proteins in 3T3-L1 adipocytes*. PLA was performed using the Duolink® system (Sigma-Aldrich) according to the manufacturer's instructions. (1) 3T3-L1 adipocytes were grown on Labtech 8-chamber slides. Following insulin stimulation where indicated, cells were fixed with paraformaldehyde (3% [w/v]) prior to permeabilisation (0.1% [w/v] saponin) in the presence of blocking solution (2% [w/v] bovine serum albumin, 20mM glycine) for 30min. (2) Primary antibody (see Table S1 for details) incubations were performed in this BSA-GLY-SAP solution overnight at 37°C in a humidity incubator. Cells were washed using BSA-GLY-SAP prior to (3) the addition of proximity probes (provided with the kit) diluted 1/5 with BSA-GLY-SAP. Cells were incubated at 37°C in a humidity chamber for 90 min prior to washing with BSA-GLY-SAP and (4) incubation in hybridisation/ligation solution (provided by the kit) for 30 min. Cells were washed with a solution of 20mM Tris-HCl pH 7.4, containing 137mM NaCl and 0.05% [v/v] Tween-20 for 5 min prior to (5) application of the amplification/detection solution (provided with the kit) and incubation for two hours at 37°C. (6) Slides were washed thoroughly with 0.1M NaCl 0.2M in Tris-HCl pH 7.5 allowed to air dry slides and mounted with DAPI containing mounting medium (provided with the kit). PLA signals were visualized using a Zeiss LSM Pascal Exciter fluorescence system with a 100× oil immersion objective.

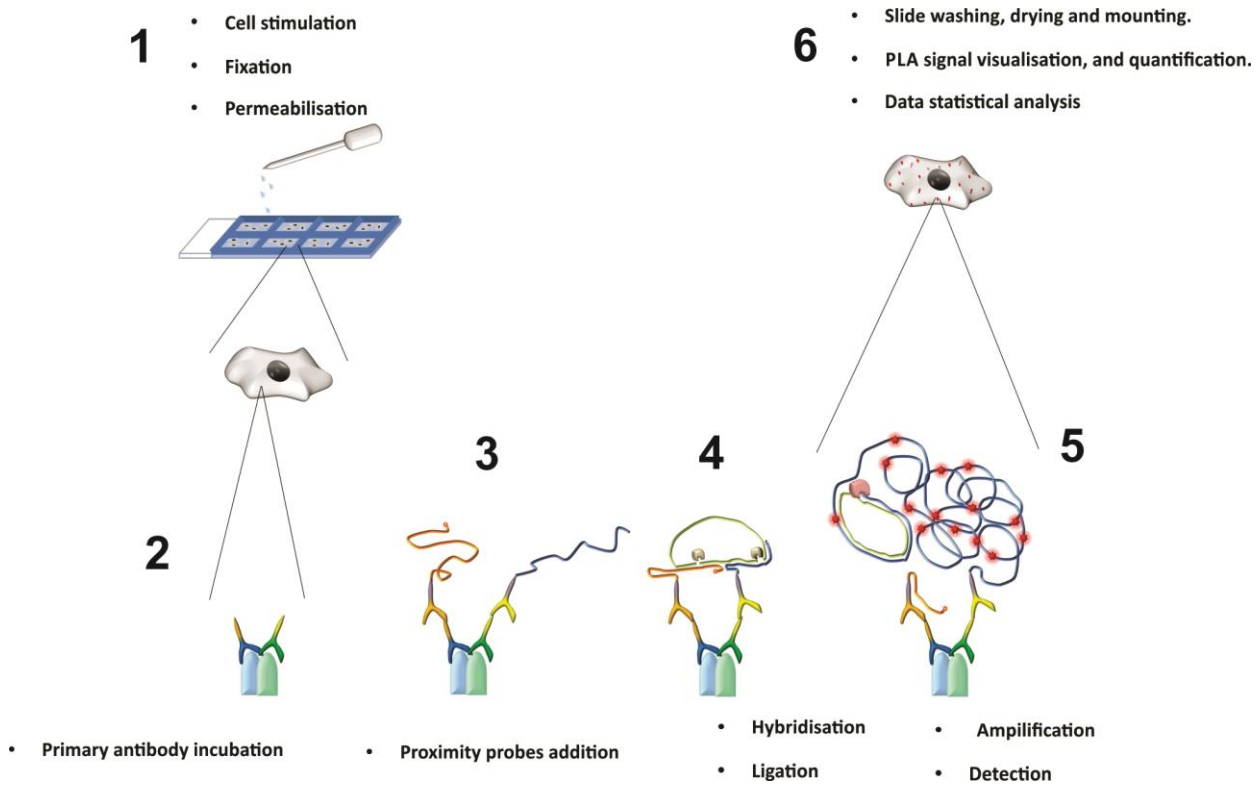

For quantification, data are presented as number of PLA puncta observed per cell (minimum of 200 cells) counted using Blobfinder version 3.2. with the following parameters used throughout: blob threshold, 120 (intensity; arbitrary units); minimum nucleus size, 100 pixels; cytoplasm size, 250 pixels; blob size, 5 by 5 pixels (i.e. in order for a puncta to be scored as a PLA signal and distinguish it from background fluorescence it must satisfy two these two parameters: blob threshold in arbitrary units and blob size in pixels, which define the minimum intensity and the minimum size respectively of a blob).

Statistical analysis of the PLA results was performed using the Mann-Whitney U test (SPSS software). Box plots presented display median values of signal per condition (from the number of cell stated, typically 200-300 cells) as well as the ranges of the values quartiles. The lower line illustrates the range of the first quartile of the sample values obtained (25% of the total number of the sample values), the box demonstrates the range of the second quartile of the values (50% of the total number) and the upper line the range of the third quartile of the values obtained. The black line in the boxes represents the median value of the samples analysed. Figures and plots are representative of the results of 3 independent experiments in all cases.

Figure S2. *Pairwise associations between Cellugyrin or Sortilin and Syntaxin4,in the presence and absence of insulin-stimulation.* PLA was used to detect pairwise associations between Cellugyrin or Sortilin and Syntaxin4 in 3T3-L1 adipocytes treated with 100nM insulin for 5 min (Insulin) or not (Basal). PLA signals are shown in red, DAPI stained nuclei in blue. Controls omitting the first listed primary antibody are shown for each pairwise combination (in all cases controls omitting either and both primary antibodies were performed in parallel and no significant signal was detected). Statistical analyses of PLA data were performed using Blobfinder and SPSS software. Boxplots represent median number of signals and quartile range of 30-50 cells per condition (y-axis; blue = basal, red =5 min insulin stimulation). Images are representative of 3 independent experiments. For all control experiments, the median PLA signal value was <1 per cell. Any median signal >1 obtained in the presence of both primary antibodies was found to be significantly greater than that obtained in controls for all combinations shown ($p < 0.001$); *** = $p < 0.001$. Scale bars = 10μm

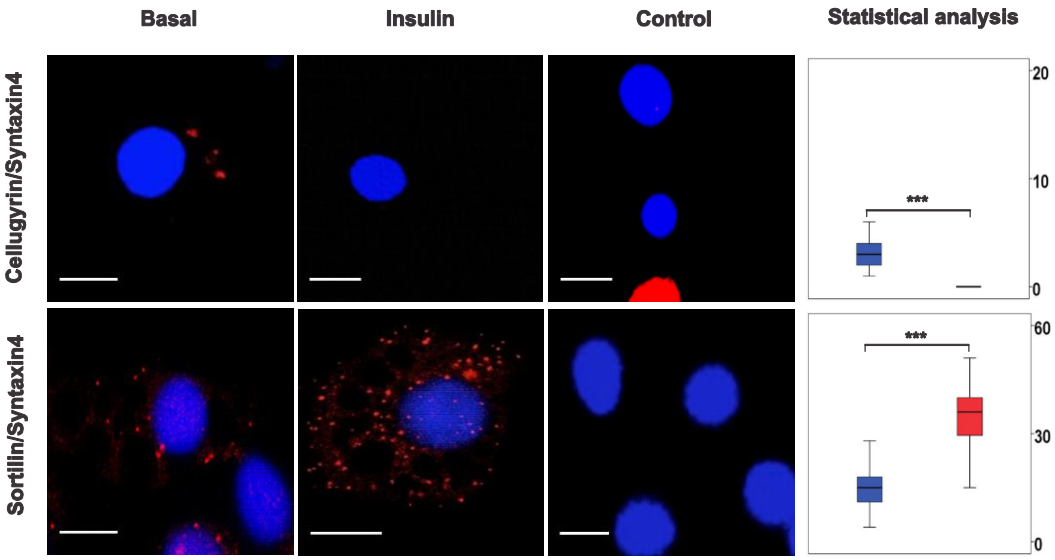

Figure S3. *Overexpression of either wild type or mutant (FDL/AAA) cellugyrin did not affect the levels of HA-GLUT4-GFP in HeLa cells.* (A) HeLa cell line stably expressing HA-GLUT4-GFP was created following infection with a lentiviral construct encoding GFP-tagged GLUT4 carrying an HA epitope in the first extracellular loop (Muretta et al., 2008). These were subsequently transiently transfected with an expression vector encoding either wild-type (WT) or mutant (FDL/AAA) tdTomato-tagged cellugyrin. Expression and localization of the tdTomato-tagged cellugyrin constructs is shown in red and the total amount of HA-GLUT4-GFP in green. Images are representative of three independent experiments. (B) Quantification of total HA-GLUT4-GFP (GFP fluorescence) of both untransfected (-) and transfected (+) cells, either with WT or FDL/AAA tdTomato-tagged cellugyrin encoding vectors, from panel A (green). The values are expressed as percentage of mean fluorescent intensity of untransfected cells. Error bars represent standard deviations from 10 different cells (data were statistically analyzed in pairs using a two-tailed t test; ns=$p \geq 0.05$). Scale bars = 10μm

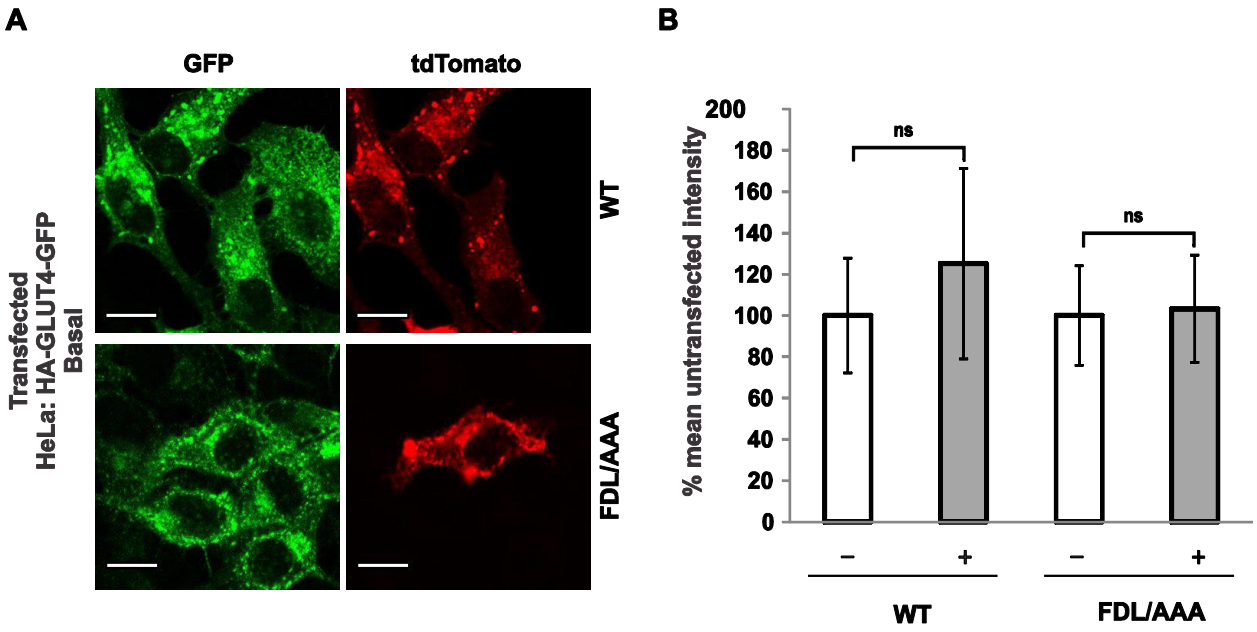

Table S1. Antibodies used in the proximity ligation assay

		Primary antibodies	
Figure	**PLA Protein pair associations**	**Mouse**	**Rabbit**
1	**Cellugyrin/Sortilin**	Anti-Cellugyrin: BD-Transduction Laboratories TM (611128); 1.25µg/ml	Anti-Sortilin: Abcam (ab16640); 5µg/ml
	Cellugyrin/VAMP2	Anti-Cellugyrin: BD-Transduction Laboratories TM (611128); 1.25µg/ml	Anti-VAMP2 : Abcam (ab18014); 5µg/ml
	Sortilin/VAMP2	Anti-VAMP2: Synaptic Systems (104211); 1:200-antiserum	Anti-Sortilin: Abcam (ab16640 ; 5µg/ml
	Cellugyrin/GLUT4	Anti-Cellugyrin: BD-Transduction Laboratories TM (611128); 1.25µg/ml	Anti-GLUT4: Synaptic Systems (235003); 2.5µg/ml
	Sortilin/GLUT4	Anti-GLUT4: Abcam (65267); 5µg/ml	Anti-Sortilin: Abcam (ab16640); 5µg/ml
2	**Cellugyrin/SNAP23**	Anti-Cellugyrin: BD-Transduction Laboratories TM (611128); 1.25µg/ml	Anti-SNAP23: Synaptic Systems (111203); 10µg/ml
	Sortilin/SNAP23	Anti-SNAP23: SantaCruz (sc-101303); 1µg/ml	Anti-Sortilin: Abcam (ab16640); 5µg/ml
3	**Cellugyrin/Munc18c**	Anti-Cellugyrin: BD-Transduction Laboratories TM (611128) ; 1.25µg/ml	Anti-Munc18c: Abcam (ab26331); 1:200-antiserum
	Sortilin/Munc18c	Anti-Munc18c: Novus Biologicals (H00006814-B01); 1:200-antiserum	Anti-Sortilin: Abcam (ab16640); 5µg/ml
S1	**Cellugyrin/Syntaxin4**	Anti-Cellugyrin: BD-Transduction Laboratories TM (611128) ; 1.25µg/ml	Anti-Syntaxin4: Synaptic Systems (110042); 1:200-antiserum
	Sortilin/Syntaxin4	Anti-Syntaxin4: BD Transduction Laboratories (610439); 1.25µg/ml	Anti-Sortilin: Abcam (ab16640); 5µg/ml